ACS OMEGA

http://pubs.acs.org/journal/acsodf

Article

Portable Heating System Based on a Liquid Metal Bath for Rapid PCR

Kangning Wang,[#] Qingran Wang,[#] Canfu Peng, Yu Guo, Yan Li, Jia Zhou, and Wenming Wu*

Cite This: *ACS Omega* 2022, 7, 26165−26173

Read Online

ACCESS | Metrics & More | Article Recommendations

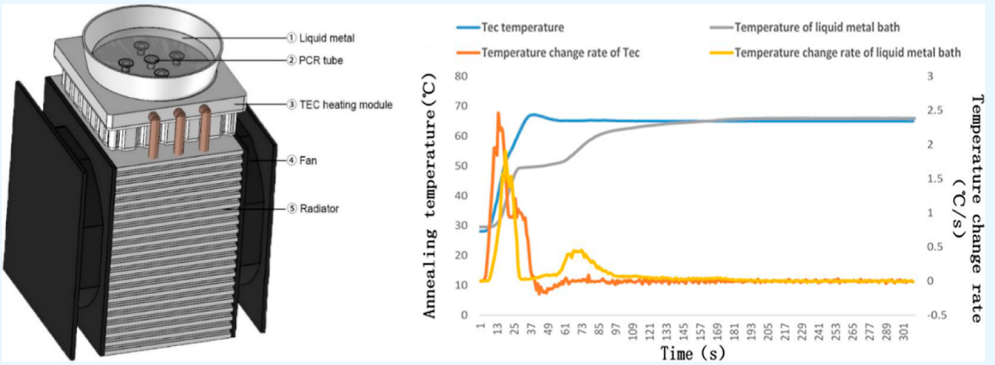

ABSTRACT: With the outbreak of COVID-19 around the world, rapid and accurate detection of new coronaviruses is the key to stop the transmission of the disease and prevent and control the novel coronavirus, among which polymerase chain reaction (PCR) is the mainstream nucleic acid detection method. A temperature cycling device is the core of the PCR amplification micro-device. The precision of the temperature control and temperature change rate directly affect the efficiency of PCR amplification. This study proposes a new PCR method based on rapid PCR chip optimization of a liquid metal bath, which realizes precise and rapid temperature rise and fall control. We systematically explored the feasibility of using liquid metals with different melting points in the system and proposed a 47 °C bismuth-based liquid metal bath as the heat conduction medium of the system to optimize the system. The heat conduction properties of the thermally conductive silicone oil bath were compared. Compared with the thermally conductive silicone oil bath, thermal cycle efficiency is improved nearly 3 times. The average heating rate of the liquid metal bath is fast, and the temperature control stability is good, which can significantly reduce the hysteresis, and the temperature change curve is more gentle, which can greatly improve the efficiency of PCR amplification. The results of gene amplification using rat DNA as the template and SEC61A as the target also indicate that the system can be successfully used in PCR devices, and the types of PCR containers can be not limited to PCR tubes. Based on the experiment, we proved that the PCR method optimized by the liquid metal bath multi-gene rapid PCR chip can further improve the temperature response speed. It has the advantages of accurate data, fast response speed, low price, safety, and environmental protection and can effectively reduce the time of PCR and improve the application efficiency. As far as we know, this is the first international report on using a liquid metal bath to do rapid-cooling PCR.

1. INTRODUCTION

The COVID-19 outbreak caused by the new coronavirus (SARS-CoV-2) infection has spread all over the world. The genetic material of the new coronavirus is a single-stranded RNA with a size of 30 kb, which is a typical RNA virus. The new crown virus is highly contagious, so fast and accurate detection of the new crown virus is the key to blocking the spread of the disease and preventing and controlling the new coronavirus epidemic.[1,2] A variety of new coronavirus nucleic acid detection methods have emerged, among which polymerase chain reaction (PCR) is the mainstream method. PCR technology has many applications in biomedical research.[3−6] PCR technology is the earliest nucleic acid amplification technology developed. Through multiple cycles of high-temperature denaturation, low-temperature annealing, and primer extension, the target can be amplified tens of thousands or even hundreds of millions of times.[7−13] As a relatively mature nucleic acid amplification technology, PCR technology has been widely used in many fields of life sciences.[14−16]

Received: March 25, 2022
Accepted: July 8, 2022
Published: July 20, 2022

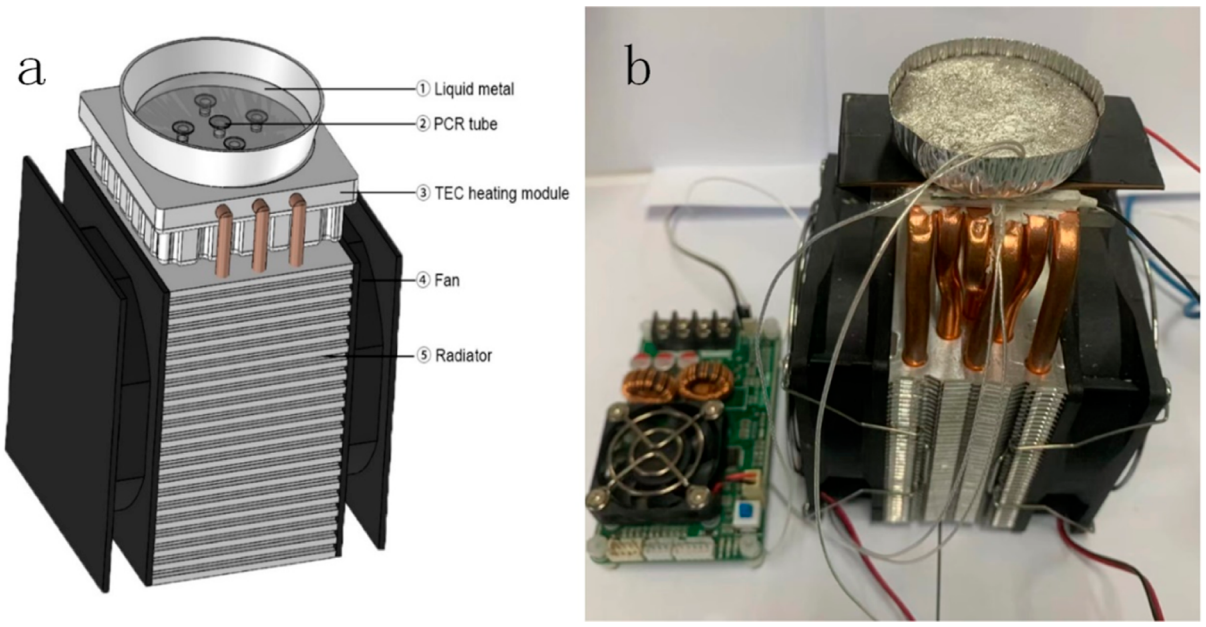

Figure 1. Schematic diagram of the overall structure of the system. (a) 3D schematic of the system and (b) physical schematic of the system.

The PCR temperature cycle is to control the temperature cycle of the sample reagents so that the nucleic acid molecules inside perform the PCR during the temperature cycle, so as to amplify the nucleic acid molecules. The temperature cycle device is the core of the PCR amplification microdevice.[17−25] The precision of the cycle temperature control and the temperature change speed directly affect the efficiency of PCR amplification. Current PCR temperature cycling devices all use indirect heating. The reagent is stored in the centrifuge tube or the chip-type flow channel, and the heating plate heats the centrifuge tube or the chip. In the process of heating the reagent, the method needs to maintain the heating state of the centrifuge tube or the chip, and there is room for further improvement in the speed of temperature response. Most of the existing PCR instrument heating modules use semiconductor heating and cooling technology or air heating and cooling technology to heat or cool the liquid in the PCR tube by means of a solid metal or oil bath for heat conduction. The temperature rise and fall speed directly affects the time consumption and effect of the PCR. PCR based on solid metal or oil baths often suffers from long detection times and is inefficient in the detection of infectious diseases such as new coronaviruses.

This study proposes a new PCR method based on liquid metal bath-based multi-gene rapid PCR chip optimization to achieve precise and rapid temperature rise and fall control, and its application is explored. Liquid metal[26−30] is a type of low-melting metal element and binary or multiple alloys, such as gallium, with a melting point near room temperature and alloys formed by gallium and one or more of indium, tin, and zinc. As a metal system with highly disordered internal microstructure arrangement, liquid metal is essentially different from conventional fluid and solid metals. In terms of macroscopic characteristics, liquid metal not only has the characteristics of easy deformation and easy flow of fluid but also has excellent thermal conductivity of metal materials. Its melting point is near room temperature. It is a kind of safe low-melting point metal material. In recent years, with the continuous in-depth and comprehensive development of liquid metal research, these advantages of liquid metal have attracted more and more attention in research and application fields. As a new type of material, liquid metal is widely used in computer chip heat dissipation, nuclear reactor cooling, and large-scale laser heat dissipation. This is mainly due to the high thermal conductivity and heat capacity of liquid metal. The thermal conductivity of a common liquid metal is generally 10−40 W/(m·K), which is 2 orders of magnitude higher than that of traditional cooling fluid water. The specific heat of liquid metals is much smaller than that of water, and the viscosity is about twice that of water, so it also has good fluidity. Liquid metal has stable chemical properties, has extremely low saturated vapor pressure and is not easy to evaporate, is easy to recycle, can be reused, and has very low loss, which can significantly save costs. Based on these excellent properties of liquid metal, we propose a PCR method based on a liquid metal bath-based multi-gene rapid PCR chip optimization, which can further improve the temperature response speed, with accurate data, fast response speed, low price, safety and environmental protection, and so forth. Advantages can effectively reduce the time-consuming PCR and improve application efficiency. Compared with the thermally conductive silicone oil bath, the thermal cycle efficiency is improved by nearly 3 times. Using rat DNA as the template and SEC61 translocon subunit alpha 1 (sec61a) as the target, we carried out the corresponding gene amplification. The experimental results proved that the system can be successfully used in the PCR device. As far as we know, this is the first report in the world that a liquid metal bath is used for rapid temperature rise and fall in PCR.

2. MATERIALS AND METHODS

Liquid metal (Dongguan Dingguan Metal Technology Co., Ltd) with melting points of 11, 16, 30, and 47 °C and dimethyl silicone oil (DOWSIL) were used to prepare a liquid metal bath and oil bath, respectively. In order to prove that the system can be successfully used in PCR devices, we added PCR tubes and two ring-shaped Teflon tubes with different inner diameters and outer diameters in the rapid cycle heating

https://doi.org/10.1021/acsomega.2c01824
ACS Omega 2022, 7, 26165−26173

Table 1. Physical Properties of Several Normal-Temperature Liquid Metals and Water

	Ga	$Ga_{75}In_{25}$	$Ga_{62.5}In_{21.5}Sn_{16}$	H_2O
melting point/°C	29.8	15.5	10.7	0
boiling point/°C	2402	2000	>1300	100
density/(g/cm^3)	6.905	6.28	6.36	1
viscosity/(Pa·s)	1.37×10^{-3}	1.99×10^{-3}	2.09×10^{-3}	1×10^{-3}
thermal conductivity/(W/m·K)	30.54	26.43	25.41	0.6
specific conductance/(S/m)	6.75×10^6	3.46×10^6	3.1×10^6	$\leq 1 \times 10^{-4}$
surface tension/(mN/m)	707	632	718	72.8

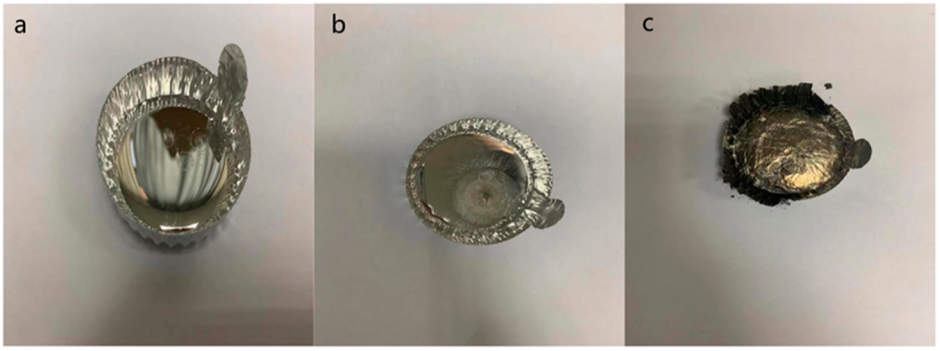

Figure 2. (a−c) Corrosive effect of the liquid metal on tin cartons over time.

and cooling equipment based on liquid metal baths (the interface is the used needle connection); using a commercial PCR cycler as a reference, four sets of experiments are set up, and the function of the system can be verified by comparing the dissolution curves of the four sets of experiments. The reaction uses rat DNA as a template and SEC61 translocon subunit alpha 1 (sec61a) as the target, and the sec61a primer sequence used for amplification is as follows: F: 5′-AGATGGGTGCTGGAATCTGC-3′ and R: 5′-CAAATTC-CATCCCTCGGCCA-3′. The configured PCR reagents consist of a 2× SYBR premix (containing PCR buffer, $MgCl_2$, dNTPs, HS Taq DNA polymerase, SYBR Green I, and a stabilizer), 22 μL of dd water (double distilled water), 1 μL of cDNA, 1 μL of forward and 1 μL of reverse primer, and a total of 50 μL of the reagent.

3. EXPERIMENTAL SECTION

We propose a new optimization method for the rapid multi-gene PCR chip based on a liquid metal bath. The overall structure of the system is shown in Figure 1. The system consists of a thermo electric cooler (TEC) heating module, radiator, fan, liquid metal bath for PCR amplification, PCR tube, and other components. The specific working process can be summarized as the following process: First, the reagents used for PCR amplification are poured into the PCR tube, and the PCR tube is sealed to ensure that there will be no sample evaporation loss or contamination during the PCR process. Then, the PCR tube is put into the liquid metal bath, the TEC heating module is controlled, and the fan is turned on. The TEC heating module is used for rapid cycle temperature change. The TEC heating module is connected to the radiator. The fans installed on both sides of the radiator are used to generate heat dissipation airflow. The radiator is used to divert the heat dissipation airflow and dissipate heat to the outside for rapid heat dissipation; the liquid metal is filled with a tin foil material because the contact surface between the tin box and the TEC heating device cannot reach the ideal flat surface; there will be air in the gap of the contact interface, and the thermal conductivity of air is very low, which will increase the interface thermal resistance and seriously affect the overall heat exchange effect. Therefore, a thermal paste is used between the tin box and the TEC heating device to fill the air gap between the heat sink and the electronic components, which is used to shorten the heat transfer path, reduce the interface contact thermal resistance, and improve the heat dissipation performance. The liquid metal bath and PCR tube located on the upper part change between different temperatures under the action of the TEC heating module's rapid cycling temperature rise and fall. Through multiple cycles of high-temperature denaturation, low-temperature annealing, and primer extension, the solution inside the PCR tube can meet the temperature change requirements of gene amplification.

3.1. Choice of the Liquid Metal Bath. In recent years, liquid metal has gradually attracted the attention of researchers due to its excellent physical properties. The liquid metal alloy matrix mainly includes gallium-based alloys, bismuth-based alloys, and their derivative metal materials. Among them, the gallium-based liquid alloy is a typical room-temperature liquid metal, which has a wide range of applications in the key refrigeration medium of the cutting-edge refrigeration field. We select the common Ga, $Ga_{75}In_{25}$, and $Ga_{62.5}In_{21.5}Sn_{16}$ for related research, and the melting points are 29.8, 15.5, 10.7 °C, respectively. The physical properties of several normal-temperature liquid metals and water are shown in Table 1.[31−35] Taking gallium as an example, we observe that it has a relatively low vapor pressure and a high boiling point, with a melting point of 29.8 °C and a boiling point of 2402 °C. Its density is 6 times that of water, its viscosity is similar to that of water, and it has good thermal conductivity (30.54 W/m·K) and chemical stability, making it a good heat transfer medium. However, Ga in the gallium-based liquid alloy bath is highly corrosive to aluminum-based materials and copper-based materials and will damage the metal cavity. We tested the corrosion effect of the liquid metal on the metal cavity over

https://doi.org/10.1021/acsomega.2c01824
ACS Omega 2022, 7, 26165−26173

time, as shown in Figure 2a,b. From the figure, we can see that the room-temperature liquid metal, which is a typical gallium-based liquid alloy, has a strong corrosive effect on the metal cavity. This hinders us from ensuring the normal long-term operation of the system and limits its application in the PCR cycle of heating and cooling.

In order to eliminate the corrosion effect of the gallium-based liquid alloy on the cavity, we chose a common bismuth-based liquid metal bath with a melting point of 47 °C for research. The composition of the bismuth-based liquid metal at 47 °C is shown in Table 2. It can be seen that the composition does not contain Ga, which will eliminate the corrosion effect on the metal cavity. In order to visually compare the performance of the gallium-based liquid alloy and bismuth-based liquid metal at 47 °C as a heat transfer medium, we conducted related experiments. $Ga_{62.5}In_{21.5}Sn_{16}$ (melting point 10.7 °C), $Ga_{75}In_{25}$ (melting point 15.5 °C), and the 47 °C bismuth-based liquid metal were chosen as the heat transfer medium to carry out the heating experiment in the high-temperature zone (90 °C) and low-temperature zone (65 °C). The temperature change and rate of temperature change of the TEC and liquid metal were tested.

Table 2. 47 °C Bi-Based Liquid Metal Composition

component/(%)	Bi	Pb	Sn	Cd	Others
mass fraction/(°C)	45	23	8	5	In_{19}

3.2. Performance Comparison Experiment. A liquid metal bath has good thermal conductivity, and the thermal conductivity is more than 40 times that of water. When a liquid metal bath is used as the heat transfer medium, the liquid metal has much higher thermal conductivity than non-metal fluids such as water, air, and other liquids (the thermal conductivity is between that of iron and aluminum); so it can be used as a heat transfer medium to speed up the temperature rise and fall rate of the thermal cycle. In order to visually prove the superiority of the rapid multi-gene PCR chip method based on the liquid metal bath, we use a liquid metal bath with a melting point of 47 °C and a thermally conductive silicone oil bath to circulate between the high-temperature zone (90 °C) and the low-temperature zone (65 °C). In the cooling experiment, the temperature change and heating rate of the liquid metal bath and the thermal silicone oil bath are shown in Figure 3a,b.

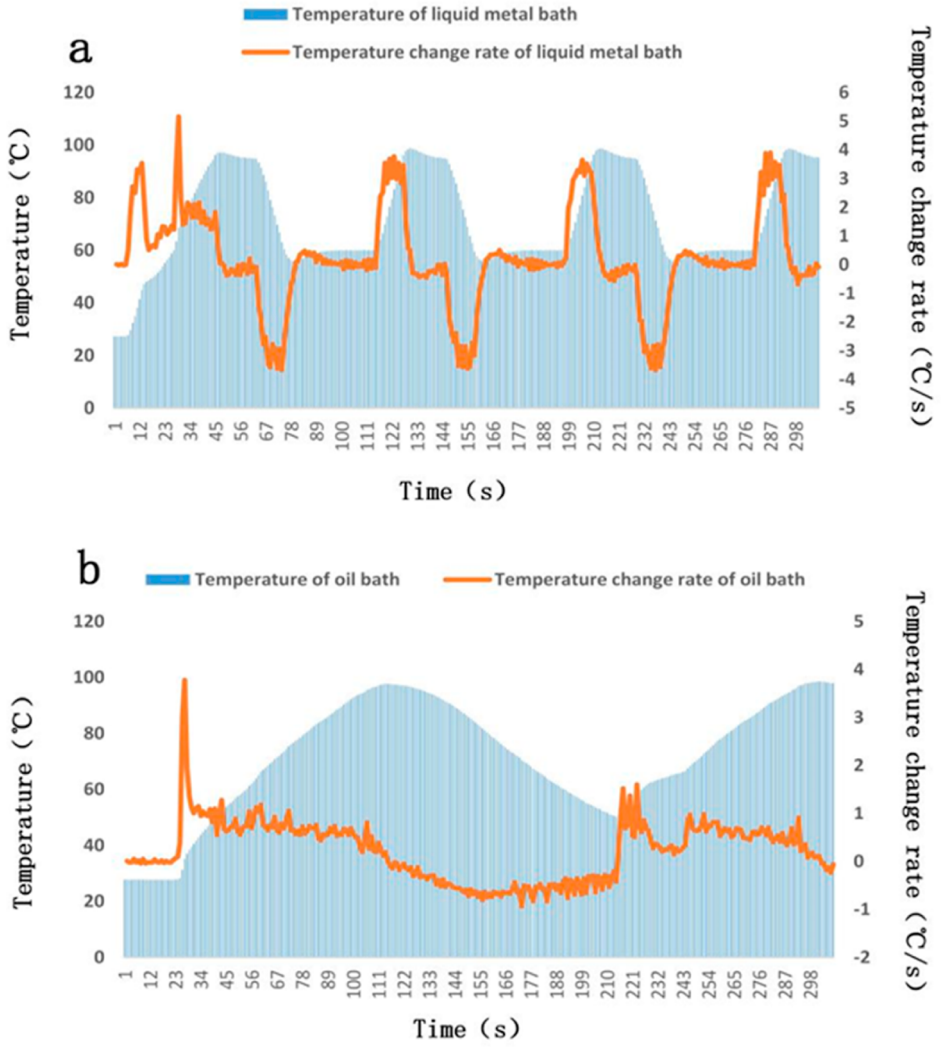

Figure 3. Liquid metal with a melting point of 47 °C and thermally conductive silicone oil are cycled between the high-temperature zone (90 °C) and the low-temperature zone (65 °C). The temperature change and heating rate of (a) liquid metal bath and (b) thermally conductive silicone oil bath.

https://doi.org/10.1021/acsomega.2c01824
ACS Omega 2022, 7, 26165−26173

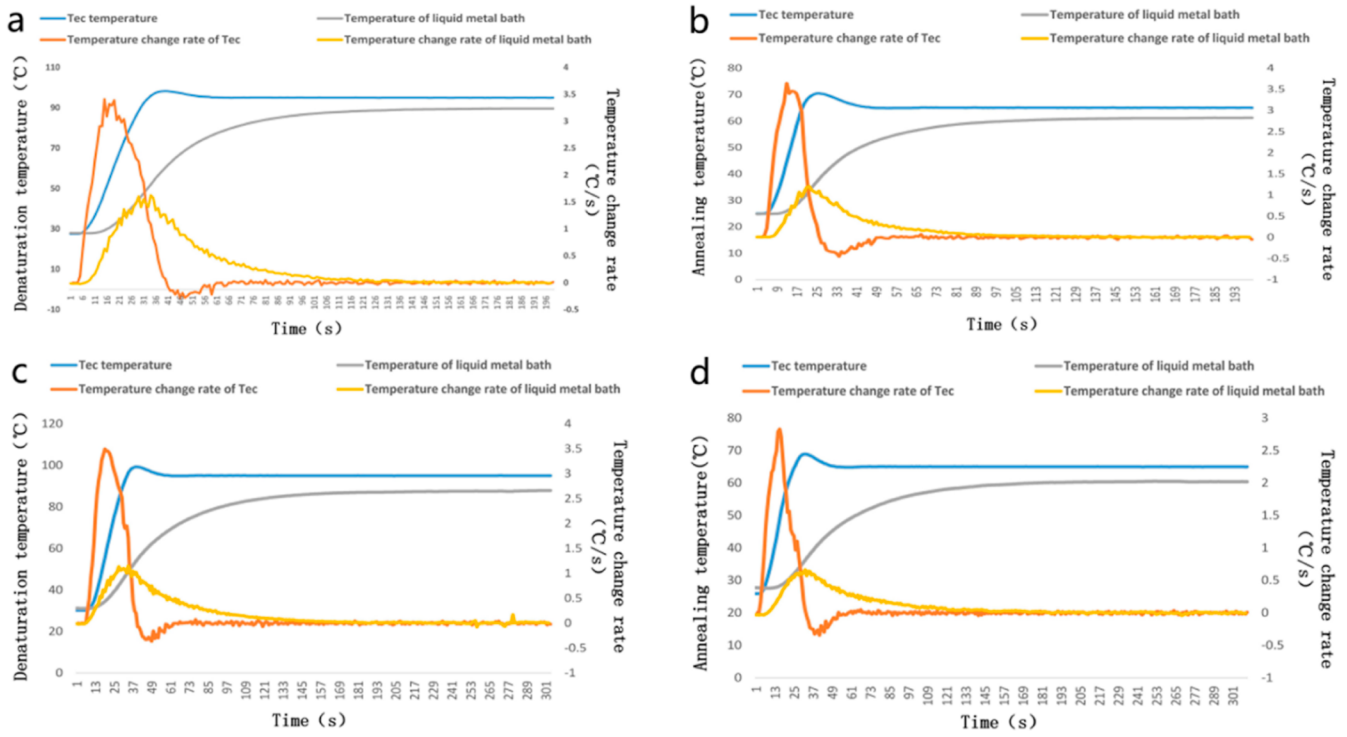

Figure 4. $Ga_{62.5}In_{21.5}Sn_{16}$ (melting point 11 °C) in high-temperature zone (90 °C) and low-temperature zone (65 °C) heating rate graphs (a,b). Diagrams (c,d) of the heating rate of $Ga_{75}In_{25}$ (melting point 16 °C) in the high-temperature zone (90 °C) and low-temperature zone (65 °C).

From the figure, we can know that in the same 300 s, the liquid metal bath can complete nearly four cycles of heating and cooling, while the thermally conductive silicone oil bath can only complete 1.5 cycles, and the thermal cycle efficiency is nearly 3 times different. The temperature cycle device is the core of the PCR amplification microdevice. Because the temperature required to realize the PCR amplification reaction comes from the heat transfer of the heat transfer medium, the precision of the cycle temperature control and the temperature change rate directly affect the efficiency of the PCR amplification. Compared with the thermally conductive silicone oil bath, the liquid metal bath has a faster average heating rate and good temperature control stability and can significantly reduce the hysteresis, and the temperature change curve is smoother, which can greatly improve the efficiency of PCR amplification. Based on experiments, we prove that the optimization method of the fast multi-gene PCR chip based on the liquid metal bath can further improve the speed of temperature response and has the advantages of accurate data, fast response, low price, safety, and environmental protection and can effectively reduce the time consumption of PCR and improve application efficiency.

4. RESULTS AND DISCUSSION

4.1. Analysis of the Temperature Change Rate of the Normal-Temperature Liquid Metal. By performing temperature-changing experiments on $Ga_{62.5}In_{21.5}Sn_{16}$ (melting point is 11 °C) and $Ga_{75}In_{25}$ (melting point is 16 °C), we have obtained the heating rate graphs in the high-temperature zone (90 °C) and low-temperature zone (65 °C), as shown in Figure 4a–d. The data shows that the $Ga_{62.5}In_{21.5}Sn_{16}$ liquid metal bath with a melting point of 11 °C has a maximum heating rate of 1.21 °C/s in the high-temperature zone (90 °C) and 1.62 °C/s in the low-temperature zone (65 °C). The maximum heating rate of the $Ga_{75}In_{25}$ liquid metal bath with a melting point of 16 °C in the high-temperature zone (90 °C) is 1.146 °C/s, and the maximum heating rate in the low-temperature zone (65 °C) is 0.66 °C/s. The temperature change rate of TEC is about 3 °C/s. Due to the good thermal conductivity and chemical stability of liquid metal, it can be a good heat transfer medium. However, since Ga in the gallium-based liquid alloy is corrosive, the cavity material must be chemically stable and will not react with the liquid metal to ensure the normal operation of the system. In the past, plexiglass or ceramic was often used as a cavity for holding the liquid metal. However, the thermal conductivity of these materials is not good, which does not meet the demand for rapid cycling and temperature rise.

4.2. Experimental Analysis of the Temperature Change Rate of the Bismuth-Based Liquid Metal with a Melting Point of 47 °C. Bi-based liquid metal and gallium-based liquid metal have the same excellent physical properties. Also, there is no corrosive effect on the cavity material, which can make the system run stably and efficiently for a long time. When used as a heat transfer medium, it uses its own low melting point to absorb the heat of the heating element. When the temperature reaches a certain level, it will become liquid, and it can always remain liquid in the working temperature range. The temperature change rate diagram of the bismuth-based liquid metal bath with a melting point of 47 °C in the high-temperature zone (90 °C) and low-temperature zone (65 °C) is shown in Figure 5a,b. It can be seen from the figure that the maximum heating rate in the high-temperature zone is 2.48 °C/s, and the maximum heating rate in the low-temperature zone is 1.91 °C/s, and the thermal conductivity is better than that of liquid metals with melting points of 11 and 16 °C. The 47 °C bismuth-based liquid metal has high thermal

https://doi.org/10.1021/acsomega.2c01824
ACS Omega 2022, 7, 26165−26173

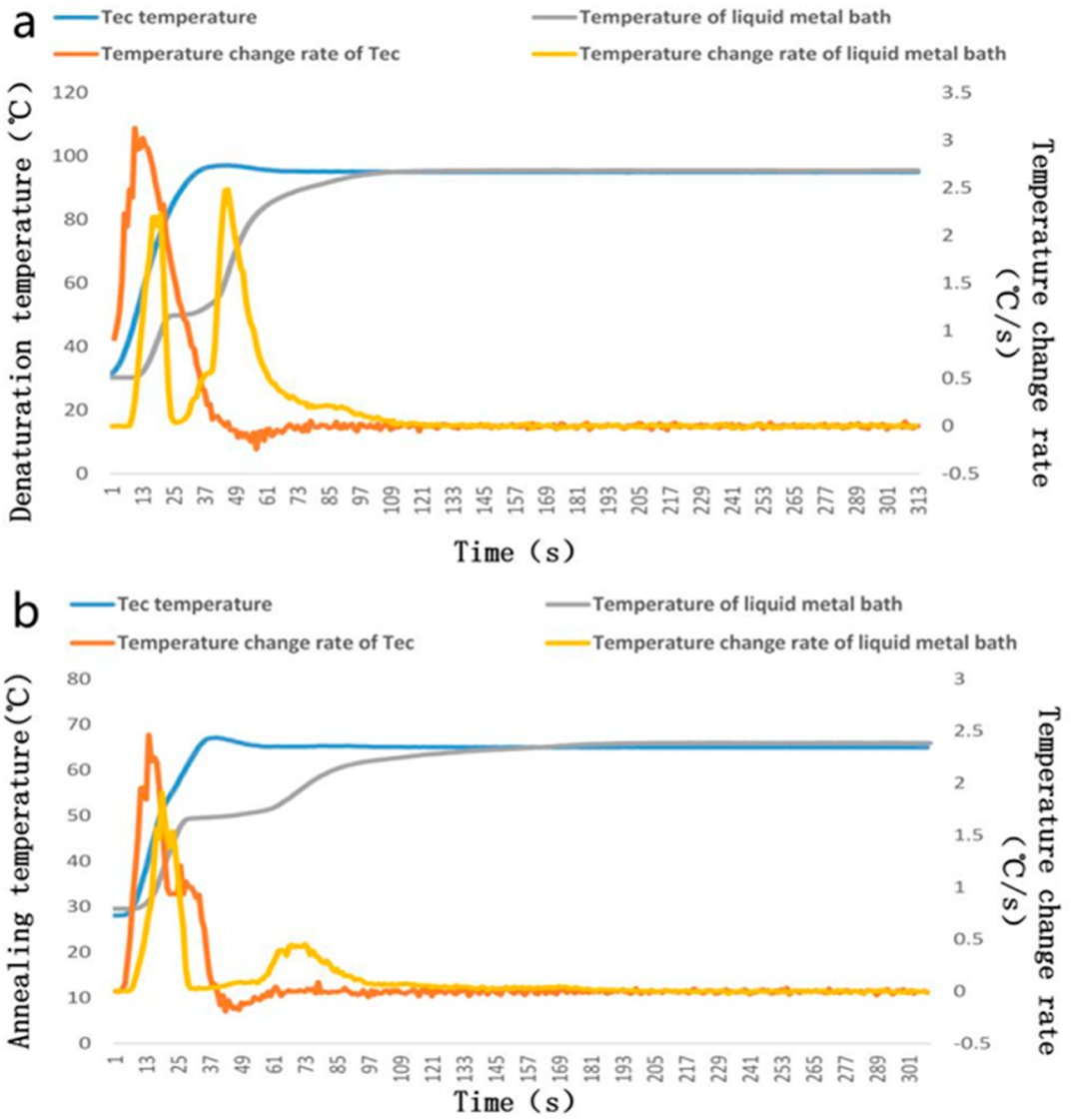

Figure 5. Temperature change rate diagram of the bismuth-based liquid metal bath with a melting point of 47 °C in (a) high-temperature zone (90 °C) and (b) low-temperature zone (65 °C).

conductivity, so it can be used as a heat transfer medium to speed up the temperature rise and fall rate of the thermal cycle.

By quantitatively comparing the temperature change rates of the common gallium-based liquid metal bath (melting point: 11, 16, and 30 °C) and bismuth-based liquid metal bath (47 °C), we found that the bismuth-based liquid metal bath with a melting point of 47 °C can always remain liquid in the working temperature range and has better heat conduction performance than the gallium-based liquid metal and will not corrode cavity materials, and the price is cheaper than that of the gallium-based liquid metal. It is worth noting that the 47 °C bismuth-based liquid metal is solid at room temperature, which is convenient for storage and recovery. It has stable chemical properties and extremely low saturated vapor pressure and is not easy to evaporate. It is environmentally friendly and non-toxic and reusable with low loss, which can significantly save costs. Based on the above-mentioned analysis, our system selects the 47 °C bismuth-based liquid metal bath as the heat conduction medium of the system. In this study, a new optimization method of a multi-gene rapid PCR chip based on a liquid metal bath is proposed to realize accurate and rapid temperature rise and fall control.

4.3. Melting Curve. In order to prove that the system can be successfully used in PCR devices, a rapid cyclic heating and cooling device based on a liquid metal bath, using a commercial qPCR cycler as a reference, was used to set up an experiment and verify the function of the system by comparing the melting curves. PCR consists of three basic reaction steps: denaturation, annealing, and extension. This reaction process is carried out in the PCR vessel. With the development of PCR technology, PCR containers generally use special thin-walled, transparent 0.2 mL PCR tubes. The dedicated PCR tube has an extremely thin tube wall and a high degree of uniformity, which has good thermal conductivity, rapid response, and uniform thermal conductivity. However, the high performance requirements of the dedicated PCR tube make it more expensive and inconvenient to obtain materials. Based on our proposed system, we propose to replace experiments with commonly used materials such as Teflon tubes. The diagram of the experimental equipment based on the liquid metal bath is shown in Figure 6a. A PCR tube and

https://doi.org/10.1021/acsomega.2c01824
ACS Omega 2022, 7, 26165−26173

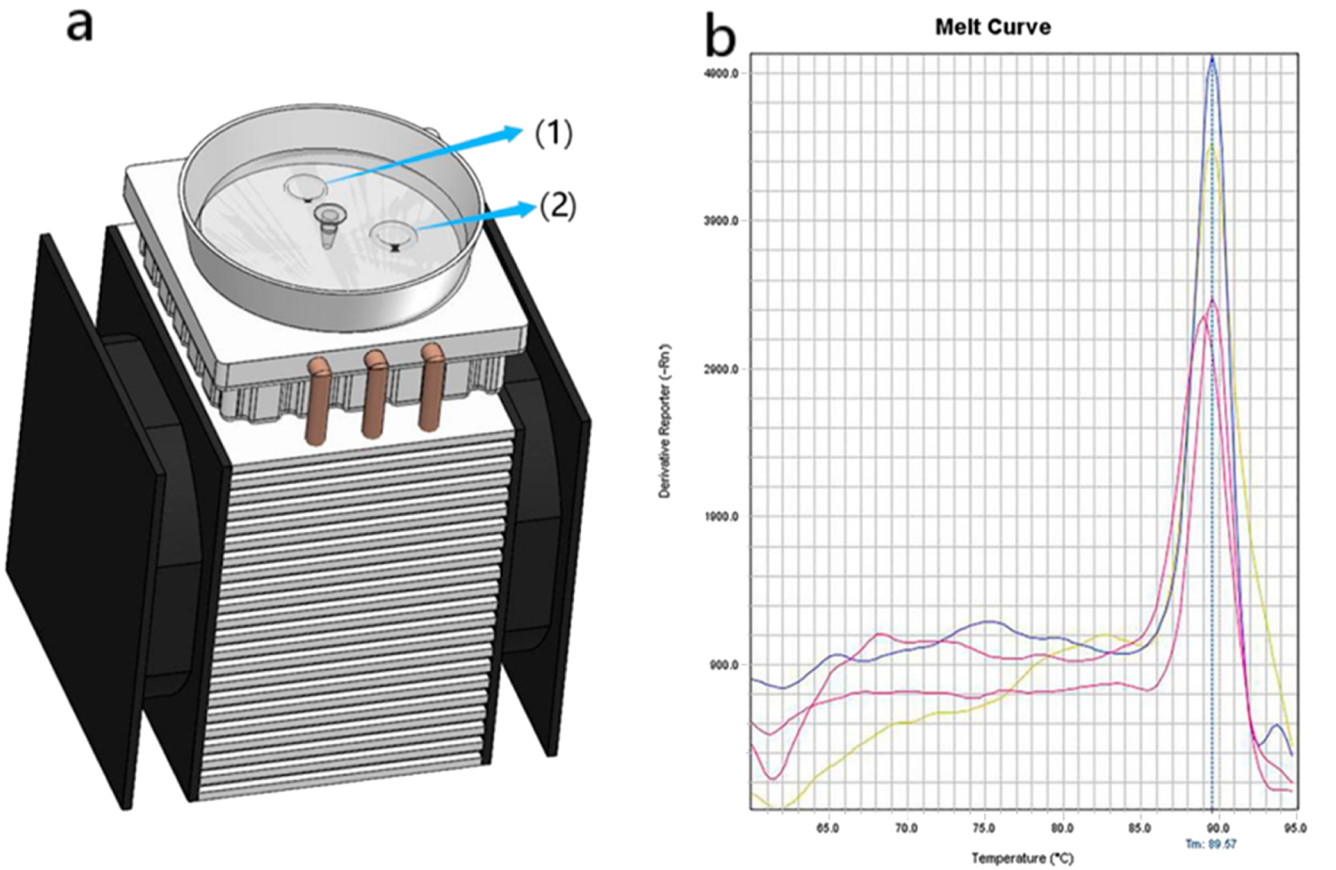

Figure 6. Experimental equipment diagram (a). A PCR tube and two ring-shaped Teflon tubes with different inner and outer diameters are placed in a liquid metal bath, using a commercial qPCR cycler as a reference. Comparison of the melting curves of the four groups of experiments (b).

two circular Teflon tubes with different inner and outer diameters are placed in the liquid metal bath, using a commercial PCR cycler as a reference. Teflon tube (1) has an inner diameter of 0.3 mm and an outer diameter of 0.6 mm, and Teflon tube (2) has an inner diameter of 0.5 mm and an outer diameter of 0.9 mm. The dissolution curves of the four groups of experiments are shown in Figure 6b. The blue curve is the melting curve of the commercial PCR cycler, the yellow curve is the melting curve based on the PCR tube, and the pink curve is the melting curve based on the two circular Teflon tubes. The abscissa of the curve is temperature, and the ordinate is the change in fluorescence intensity. It can be seen from the figure that the product produced by the commercial qPCR cycler is consistent with the test result of the experimental product produced by our equipment. Therefore, this new method can achieve the amplification of DNA fragments such as sec61a with higher amplification efficiency. A commercial qPCR cycler and PCR optimized for a multi-gene rapid PCR chip based on a liquid metal bath produce products with the same composition and two circular Teflon tubes with different inner and outer diameters. A similar amplification effect is also achieved, which shows that the types of PCR containers can be expanded, the price can be reduced, and materials can be easily obtained. The amplification efficiency of the four sets of experiments is similar, which means that the system can be used for PCR applications.

5. CONCLUSIONS

This study proposes a new optimization method for a rapid multi-gene PCR chip based on a liquid metal bath, which realizes accurate and rapid temperature rise and fall control. The use of liquid metal as the heat transfer medium which has a thermal conductivity much higher than that of water, air, and many non-metallic media can greatly improve the heat transfer efficiency. Liquid metal is small, hard to volatilize, less sensitive to the environment, easy to recycle, and reusable and has extremely low loss, which can also ensure safety, extend the service life of the equipment, and reduce costs. We systematically explored the feasibility of applying liquid metals with different melting points to this system and compared the thermal conductivity with that of thermally conductive silicone oil baths. Compared with the thermally conductive silicone oil bath, the thermal cycle efficiency is improved by nearly 3 times. The liquid metal bath has a fast average heating rate and good temperature control stability, which can significantly reduce the hysteresis, and the temperature change curve is smoother, which can greatly improve the efficiency of PCR amplification. The gene amplification results also show that the system can be successfully used in PCR devices, and the PCR container may not be limited to PCR tubes. Based on experiments, we prove that the optimization method of a fast multi-gene PCR chip based on a liquid metal bath further improves the speed of temperature response. It has the advantages of accurate data, fast response, low price, safety and environmental protection, and so forth, which can effectively reduce the time consumption of PCR and improve application efficiency.

https://doi.org/10.1021/acsomega.2c01824
ACS Omega 2022, 7, 26165−26173

AUTHOR INFORMATION

Corresponding Author

Wenming Wu − *Institute of Biological and Medical Engineering, Guangdong Academy of Sciences, Guangzhou 516001, China;* orcid.org/0000-0003-4793-6132; Email: wuwenming627@163.com

Authors

Kangning Wang − *Institute of Biological and Medical Engineering, Guangdong Academy of Sciences, Guangzhou 516001, China*

Qingran Wang − *State Key Laboratory of Luminescence and Applications, Changchun Institute of Optics, Fine Mechanics and Physics, Chinese Academy of Sciences, Changchun 130033, China; Center of Materials Science and Optoelectronics Engineering, University of Chinese Academy of Sciences, Beijing 100049, China*

Canfu Peng − *State Key Laboratory of Luminescence and Applications, Changchun Institute of Optics, Fine Mechanics and Physics, Chinese Academy of Sciences, Changchun 130033, China; Center of Materials Science and Optoelectronics Engineering, University of Chinese Academy of Sciences, Beijing 100049, China*

Yu Guo − *School of Mechanical and Electrical Engineering, Guangdong University of Technology, Guangzhou 510006, China*

Yan Li − *Institute of Biological and Medical Engineering, Guangdong Academy of Sciences, Guangzhou 516001, China*

Jia Zhou − *State Key Laboratory of Microelectronics and Integrated Circuits, Fudan University, Shanghai 200433, China*

Complete contact information is available at: https://pubs.acs.org/10.1021/acsomega.2c01824

Author Contributions

#K.W. and Q.W. contributed equally to this work.

Funding

This project is supported by GDAS′ Project of Science and Technology Development (2022GDASZH-2022010110) and the State Key Laboratory of ASIC and System, Fudan University, with grant no. 2020KF005.

Notes

The authors declare no competing financial interest.

REFERENCES

(1) Yuan, X.; Yang, C.; He, Q.; Chen, J.; Yu, P.; Li, J.; Zhai, S.; Qin, Z.; Du, K.; Chu, Z.; Qin, P. Current and Perspective Diagnostic Techniques for COVID-19. *ACS Infect. Dis.* **2020**, *6*, 1998−2016.

(2) Shang, Z.; Chan, S. Y.; Liu, W. J.; Li, P.; Huang, W. Recent Insights into Emerging Coronavirus: SARS-CoV-2. *ACS Infect. Dis.* **2020**, *7*, 1369−1388.

(3) Ma, F.; Liu, M.; Zhang, C.-y.; Tang, B. Sensitive Quantification of MicroRNAs by Isothermal Helicase-Dependent Amplification. *Anal. Chem.* **2017**, *89*, 6182−6187.

(4) Li, C. C.; Chen, H. Y.; Luo, X.; Hu, J.; Zhang, C. Y. Multicolor fluorescence encoding of different microRNAs in lung cancer tissues at the single-molecule level. *Chem. Sci.* **2021**, *12*, 12407−12418.

(5) Wang, Z.-y.; Li, D.-l.; Tian, X.; Zhang, C.-y. A copper-free and enzyme-free click chemistry-mediated single quantum dot nanosensor for accurate detection of microRNAs in cancer cells and tissues. *Chem. Sci.* **2021**, *12*, 10426−10435.

(6) Wang, L.-j.; Lu, Y.-y.; Zhang, C.-y. Construction of self-directed replication system for label-free and real-time sensing of repair glycosylases with zero background. *Chem. Sci.* **2019**, *11*, 587−595.

(7) Valasek, M. A.; Repa, J. J. The power of real-time PCR. *Adv. Physiol. Educ.* **2005**, *29*, 151.

(8) Crews, N.; Wittwer, C.; Gale, B. Thermal gradient PCR in a continuous-flow microchip. *Proceedings of Spie the International Society for Optical Engineering*, 2007; Vol. *6465*(2), pp 187−195.

(9) Crews, N.; Wittwer, C.; Palais, R.; Gale, B. Product differentiation during continuous-flow thermal gradient PCR. *Lab Chip* **2008**, *8*, 919−924.

(10) Depuydt, C. E.; Benoy, I. H.; Bailleul, E. J.; Vandepitte, J.; Vereecken, A. J.; Bogers, J. J. Improved endocervical sampling and HPV viral load detection by Cervex-Brush Combi. *Cytopathology* **2010**, *17*, 374−381.

(11) Saiki, R.; Gelfand, D.; Stoffel, S.; Scharf, S.; Higuchi, R.; Horn, G.; Mullis, K.; Erlich, H. Primer-directed enzymatic amplification of DNA with a thermostable DNA polymerase. *Science* **1988**, *239*, 487−491.

(12) Erlich, H. A. Polymerase chain reaction. *J. Clin. Immunol.* **1989**, *9*, 437.

(13) Mullis, K. Target amplification for DNA analysis by the polymerase chain reaction. *Ann. Biol. Clin.* **1990**, *48*, 579−582.

(14) Lee, Y.; Kang, B.-H.; Kang, M.; Chung, D. R.; Yi, G.-S.; Lee, L. P.; Jeong, K.-H. Nanoplasmonic on-chip PCR for rapid precision molecular diagnostics. *ACS Appl. Mater. Interfaces* **2020**, *12*, 12533−12540.

(15) Mocellin, S.; Rossi, C. R.; Pilati, P.; Nitti, D.; Marincola, F. M. Quantitative real-time PCR: a powerful ally in cancer research. *Trends Mol. Med.* **2003**, *9*, 189−195.

(16) Liu, Y.; Wu, H.; Zhou, Q.; Song, Q.; Rui, J.; Zou, B.; Zhou, G. Digital quantification of gene methylation in stool DNA by emulsion-PCR coupled with hydrogel immobilized bead-array. *Biosens. Bioelectron.* **2017**, *92*, 596−601.

(17) Kopp, M. U.; de Mello, A. J.; Manz, A. Chemical amplification: continuous-flow PCR on a chip. *Science* **1998**, *280*, 1046−1048.

(18) Moschou, D.; Vourdas, N.; Kokkoris, G.; Papadakis, G.; Parthenios, J.; Chatzandroulis, S.; Tserepi, A. All-plastic, low-power, disposable, continuous-flow PCR chip with integrated microheaters for rapid DNA amplification. *Sens. Actuators, B* **2014**, *199*, 470−478.

(19) Ha, M. L.; Lee, N. Y. Miniaturized polymerase chain reaction device for rapid identification of genetically modified organisms. *Food Control* **2015**, *57*, 238−245.

(20) Jeong, S.; Lim, J.; Kim, M.-Y.; Yeom, J.; Cho, H.; Lee, H.; Shin, Y.-B.; Lee, J.-H. Portable low-power thermal cycler with dual thin-film Pt heaters for a polymeric PCR chip. *Biomed. Microdevices* **2018**, *20*, 14.

(21) Chen, J. J.; Liao, M. H.; Li, K. T.; Shen, C. M. One-heater flow-through polymerase chain reaction device by heat pipes cooling. *Biomicrofluidics* **2015**, *9*, 014107.

(22) Wu, W.; Lee, N. Y. Three-dimensional on-chip continuous-flow polymerase chain reaction employing a single heater. *Anal. Bioanal. Chem.* **2011**, *400*, 2053−2060.

(23) Schaerli, Y.; Wootton, R. C.; Robinson, T.; Stein, V.; Dunsby, C.; Neil, M. A.; French, P. M.; deMello, A. J.; Abell, C.; Hollfelder, F. Continuous-flow polymerase chain reaction of single-copy DNA in microfluidic microdroplets. *Anal. Chem.* **2009**, *81*, 302−306.

(24) Jiang, L.; Mancuso, M.; Lu, Z.; Akar, G.; Cesarman, E.; Erickson, D. Solar thermal polymerase chain reaction for smartphone-assisted molecular diagnostics. *Sci. Rep.* **2014**, *4*, 4137.

(25) Li, Y.; Zhang, C.; Xing, X. Fast identification of foodborne pathogenic viruses using continuous-flow reverse transcription-PCR with fluorescence detection. *Microfluid. Nanofluid.* **2011**, *10*, 367−380.

(26) Deng, Y.; Jiang, Y.; Liu, J. Low-melting-point liquid metal convective heat transfer: A review. *Appl. Therm. Eng.* **2021**, *193*, 117021.

(27) Miner, A.; Ghoshal, U. Cooling of high-power-density microdevices using liquid metal coolants. *Appl. Phys. Lett.* **2004**, *85*, 506−508.

(28) Ghoshal, U.; Grimm, D.; Ibrani, S.; Johnston, C.; Miner, A. High-performance liquid metal cooling loops. *Semiconductor Thermal*

Measurement and Management IEEE Twenty First Annual IEEE Symposium; IEEE, 2005; pp 16−19.
(29) Deng, Y.; Liu, J. Design of Practical Liquid Metal Cooling Device for Heat Dissipation of High Performance CPUs. *J. Electron. Packag.* **2010**, *132*, 031009.
(30) Ma, K. Q.; Liu, J. Nano liquid-metal fluid as ultimate coolant. *Phys. Lett. A* **2007**, *361*, 252−256.
(31) Briggs, L. J.; Lyman, J. Gallium: Thermal Conductivity; Supercooling; Negative Pressure. *J. Chem. Phys.* **1957**, *26*, 784−786.
(32) Liu, T.; Sen, P.; Kim, C.-J. Characterization of Nontoxic Liquid-Metal Alloy Galinstan for Applications in Microdevices. *J. Microelectromech. Syst.* **2012**, *21*, 443−450.
(33) Plevachuk, Y.; Sklyarchuk, V.; Eckert, S.; Gerbeth, G.; Novakovic, R. Thermophysical Properties of the Liquid Ga-In-Sn Eutectic Alloy. *J. Chem. Eng. Data* **2014**, *59*, 757−763.
(34) Morley, N.; Burris, J.; Cadwallader, L.; Nornberg, M. GaInSn usage in the research laboratory. *Rev. Sci. Instrum.* **2008**, *79*, 056107.
(35) Moskalyk, R. R. Gallium: the backbone of the electronics industry. *Miner. Eng.* **2003**, *16*, 921−929.

https://doi.org/10.1021/acsomega.2c01824
ACS Omega 2022, 7, 26165−26173